Extreme wind atlases of South Africa from global reanalysis data

Larsén, Xiaoli Guo; Kruger, Andries; Badger, Jake; Ejsing Jørgensen, Hans

Published in:
Proceeding of the 6th European African Conference on Wind Engineering

Publication date:
2013

Extreme wind atlases of South Africa from global reanalysis data

Xiaoli Guo Larsén[1], Andries Kruger[2], Jake Badger[1] and Hans E. Jørgensen[1]

[1]Wind Energy Department, Risø Campus, Technical University of Denmark, Roskilde.

xgal@dtu.dk

[2]Climate Service, South African Weather Service, Pretoria East, South Africa.

Abstract

Extreme wind atlases of South Africa were developed using three reanalysis data and recently developed approaches. The results are compared with the maps produced using standard wind measurements over the region. It was found that different reanalyses with the same approach provide similar spatial distribution of the extreme wind with coarse resolution data giving smaller extreme winds. The CFSR surface winds at 38 km horizontal resolution provides the best spatial distribution of the extreme winds.

1 Introduction

Extreme winds in South Africa have been studied extensively through measurements (e.g. Kruger 2010, Kruger *et al.* 2010). While measurements may suffer from technical inconsistency through time and the spatial coverage is sometimes limited for producing the extreme wind maps, the reanalysis data have been produced in light of these issues. This study uses a variety of reanalysis products and several recently developed methodologies to calculate the extreme wind atlases over South Africa. Three reanalysis data are used: the NCEP-DOE reanalysis II, the ERA-40 and the CFSR data (Section 3). This provides an insight of the range of the extreme wind estimations. The extreme wind here is defined as the 50-year wind of hourly temporal resolution at 10 m height. Two types of 50-year winds are calculated: one is over the "actual" roughness length, such as those used in the models, and we denote it as U_{50}; the other is over a homogeneous surface with a roughness length of 5 cm, the so-called standard conditions, and we denote it as $U_{50,st}$. The use of the standard condition not only provides a platform for comparing estimates from different data sources – be it from measurement, or from different models – it is also the condition for linking the larger scale flow to microscale modeling using the widely used software for extreme wind estimation, WAsP Engineering. The results are compared to those developed from measurements (Kruger 2010).

Here, U_{50} are calculated from the relatively fine spatial resolution data CFSR surface wind time series. For the standard condition, $U_{50,st}$, are estimated from the CFSR, NCEP-DOE reanalysis II and ERA-40 data.

2 Methods

The 50-year winds are calculated using the Annual Maximum Method (AMM), with the Gumbel distribution (Gumbel 1958). The annual maximum winds of the standard conditions are derived using two approaches as introduced in Section 2.1 and 2.2, respectively. Section 2.3 introduces the spectral correction method to correct the smoothing effect of the global data on the estimation of extreme wind. The different combinations of data and approaches are indicated in Table 1 as ID.

2.1 Approach 1: Application of geostrophic wind

The approach was described in detail in Larsén and Mann (2009). The geostrophic wind *G* at each reanalysis grid point is calculated from pressure and temperature data. We assume that the actual

surface winds share the same G as the wind that is corrected to the standard condition, and thus obtain the friction velocity u_* corresponding to the standard condition through the geostrophic drag law (Tennekes 1982): $G = \frac{u_*}{\kappa}\sqrt{\left(\ln\frac{u_*}{fz_0} - A\right)^2 + B^2}$, where the surface roughness, $z_{0,}$ is set to the standard value 0.05 m, A and B are dimensionless parameters and f is the Coriolis parameter. The standard winds can now be obtained through the surface logarithmic wind law: $u = \frac{u_*}{\kappa}\ln\frac{z}{z_0}$, where κ is the von Kamon constant.

2.2 Approach 2: Application of surface wind and a generalization procedure

For each reanalysis grid point, the annual winds are identified and corrected to the standard condition through the so-called generalization factors (see Badger *et al.* 2010 and Larsén *et al.* 2012a where the post-processing procedure was described and applied to mesoscale modelled winds). Briefly, the linear computational model, LINCOM, is used to calculate the sector-wise perturbations to the wind speed given by orography and roughness change. These perturbations are expressed as generalization factors, which are height and direction dependent.

2.3 The spectral correction method

This method was developed to add the wind variability in a certain range of frequency to the modelled time series that is missed out by the mesoscale modelling due to the smoothing effect (Larsén et al. 2012b). This smoothing effect is more severe with two of the three global reanalysis datasets as these have a relatively coarse resolution. The issue is illustrated in Fig. 1 where the power spectra from various model data are shown to miss the energy suggested by the measurements for f > 1 day^{-1}.

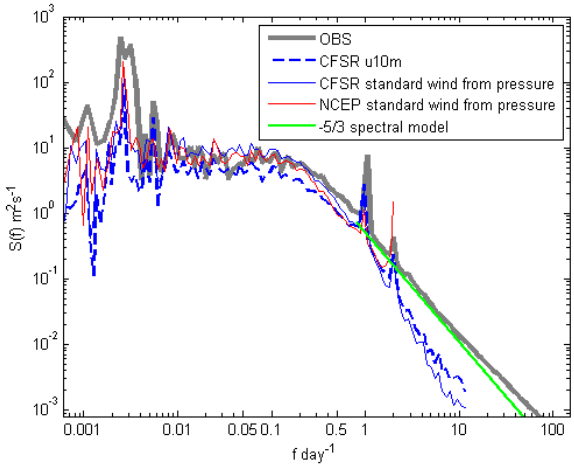

Figure 1: Power spectrum of wind speed for Cape Town from different data shown in the legend. The green curve shows a spectral model with a slope of -5/3 to a frequency of 72/day, corresponding to a time series of temporal resolution of 10 min.

Larsén *et al.* (2012b) showed that, following a Gaussian process, the annual wind maximum is a function of the second and zero order spectral moments. The missing energy in the high frequency range is particularly essential for the second order spectral moment. The underestimation in the annual wind maxima can be estimated by comparing it using the original and the modified spectrum. The replaced spectrum could be provided by measurements, if there is any, or by the spectrum model, indicated by the green curve in Fig. 1. In this case, there are no measurements for most grid points. Therefore we choose to use the spectral model. The spectrum model neglects the diurnal peak, which

could be important for over land conditions. Accordingly, we start the spectral correction from f = 1.1 day^{-1}. In order to obtain the equivalent 1 hour value with the uplifted energy, the correction ends at f = 12 day^{-1}, the Nyquist frequency of an hourly time series. In order to obtain the equivalent 10 min value with the uplifted energy, the correction ends at f = 72 day^{-1}, the Nyquist frequency of a time series with a 10 min time increment.

Figure 2 shows the spectral correction factors for correcting the hourly CFSR data (Figure 2a) and the 6 hourly NCEP data (Figure 2b) to the equivalent 1 hour value with the full uplifted spectrum.

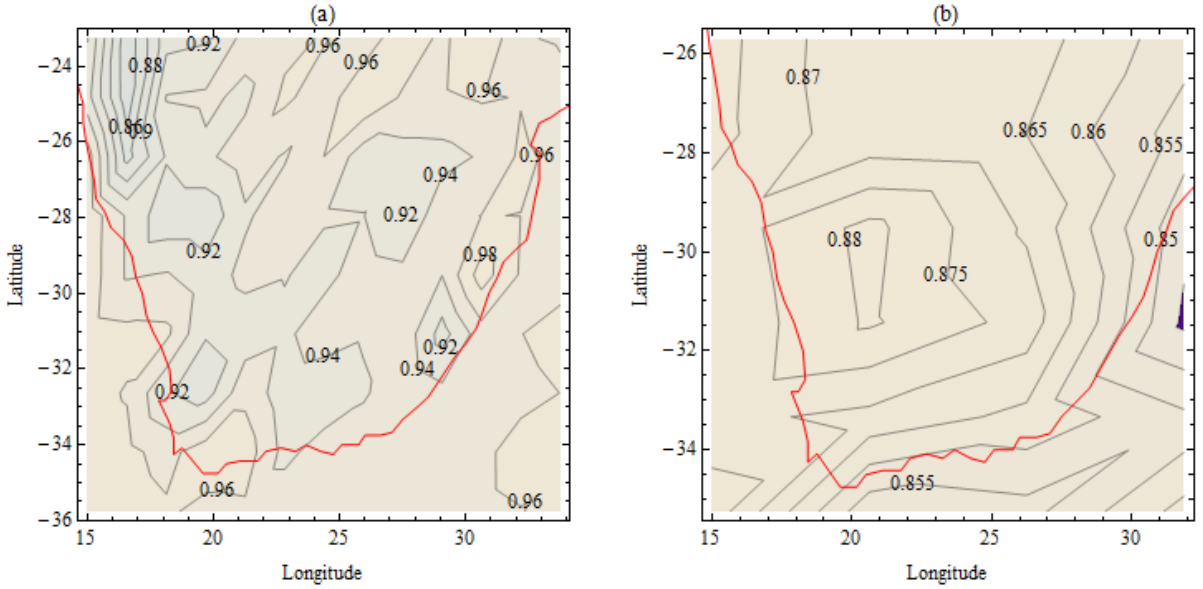

Figure 2. The spectral correction factors for (a) the CFSR wind time series, from 1 hour to 1hour and (b) 6-hourly NCEP-DOE reanalysis data, to give the corrected equivalent hourly value.

3 The global reanalysis data

Some of the details of the various reanalysis data used here are listed in Table 1. The index ID is referred to in Section 5 for the different combinations of data and approaches.

For the CFSR data, there is a considerable difference in the data assimilation before and after 1998. In Larsén 2013, there was found some inconsistency in the data before and after mid 90's over some part of the North Sea. However, it was not conclusive in Larsén 2013 where the inconsistency came from and how the inconsistency was distributed in space over the entire globe. Here, we examine the results from three periods, 1979 – 2010 (the entire time series), 1998 – 2010 (one consistent data assimilation scheme) and 1995 – 2010 (period overlapping with measurement period).

To better understand the spatial distribution of the winds, the topography and roughness length used in the CFSR reanalysis is shown in Figure 3a and b. In the CFSR reanalysis, over water, the roughness length z_0 is described through the Charnock formulation and over land it is a function of land cover and is based on a monthly climatology. The mean of the 12 monthly roughness lengths is shown in Figure 3b. These roughness lengths are higher than the actual roughness length as reported in Kruyer (2010) where for the most part of the domain it is close to 0.05 m.

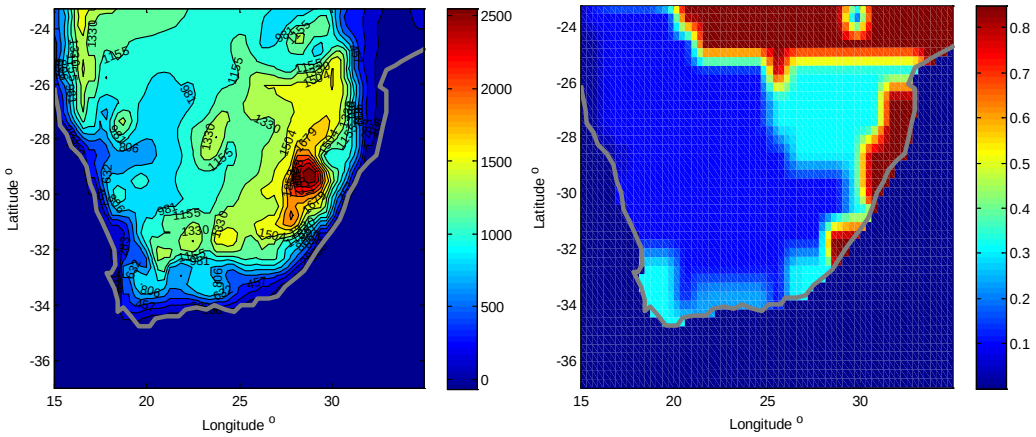

Figure 3. (a) (left plot) the surface elevation in meters and (b) (right plot) the mean of 12 monthly roughness lengths used within the CFSR reanalysis model.

Table 1: Details of the reanalysis data used in this study.

ID	Reanalysis data	Period	Spatial resolution	Temporal resolution	Variables used	Approach used
I	CFSR	1979 – 2010	38 km	1 h	u_{10}, v_{10}	2
II	CFSR	1979 – 2010	0.5 deg.	1 h	P_{msl}, T_{1000mb}	1
III	ERA-40	1958 – 2003	250 km	6 h	P_{msl}, T_{2m}	1
IV	NCEP-DOE re. II	1979 – 2010	200 km	6 h	P_{sfc}, T_{2m}	1

4 Atlases from measurements

Standard measurements of wind speed and direction at 10 m from 76 stations over South Africa were used to create the 50-year wind atlas in Kruger (2010). The atlas of 1 hour values is presented in Figure 4a. Figure 4b shows the dominant strong wind mechanisms for the hourly mean wind speed (Kruger 2010).

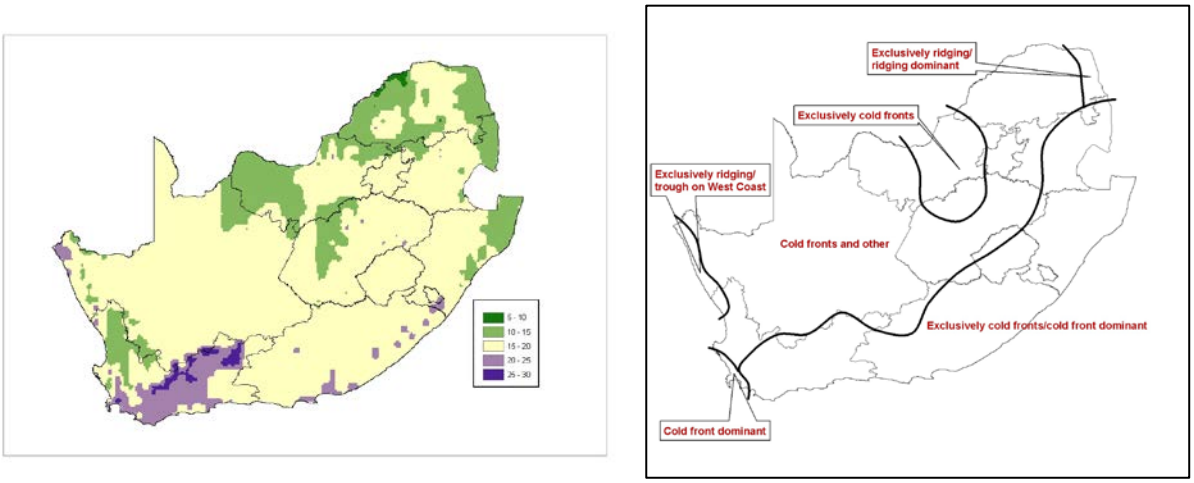

Figure 4, left (a): 50-year wind of hourly mean values based on measurements; right (b): Dominance of different strong wind mechanisms for hourly mean wind speed.

5 Results and data validation

The 50-year wind is first calculated directly from the CFSR hourly 10-metre wind time series for each grid point. The map is shown in Figure 5a. At the same time, the spectral correction factor for every 6th

grid point is calculated (section 2.3) instead of for each grid point, which saves a large amount of computation. This is a reasonable simplification since the CFSR data do not suggest considerable spatial variation of the correction factor. The spectral correction factor has been calculated for the conversion of the hourly CFSR time series with missing spectral energy in the range of $f > 1$ day^{-1} to equivalent hourly values with a full spectrum. This is done to make comparison with the result in Kruyer (2010) which was based on hourly time series. The correction factors were afterwards applied to the values as in Figure 5a and the results are shown in Figure 5b, which can now be compared to measurements (Figure 4a). Figure 5b agrees well with Figure 4a for the most, except that (1) there are missing areas where the extreme winds are in the range of 25 – 30 ms^{-1} (this could be a result of several reasons: the model data miss local extreme mechanisms such as thunderstorm, the roughness length as used in CFSR reanalysis is too large, leading to weaker winds); (2) the maxima of high winds along the high terrains (see Figure 3a) are missing in the measurement map (which could be due to the different surface conditions as for the modelled and measured data, or due to overestimation of the CFSR data or equally likely, too sparse measurements in these areas).

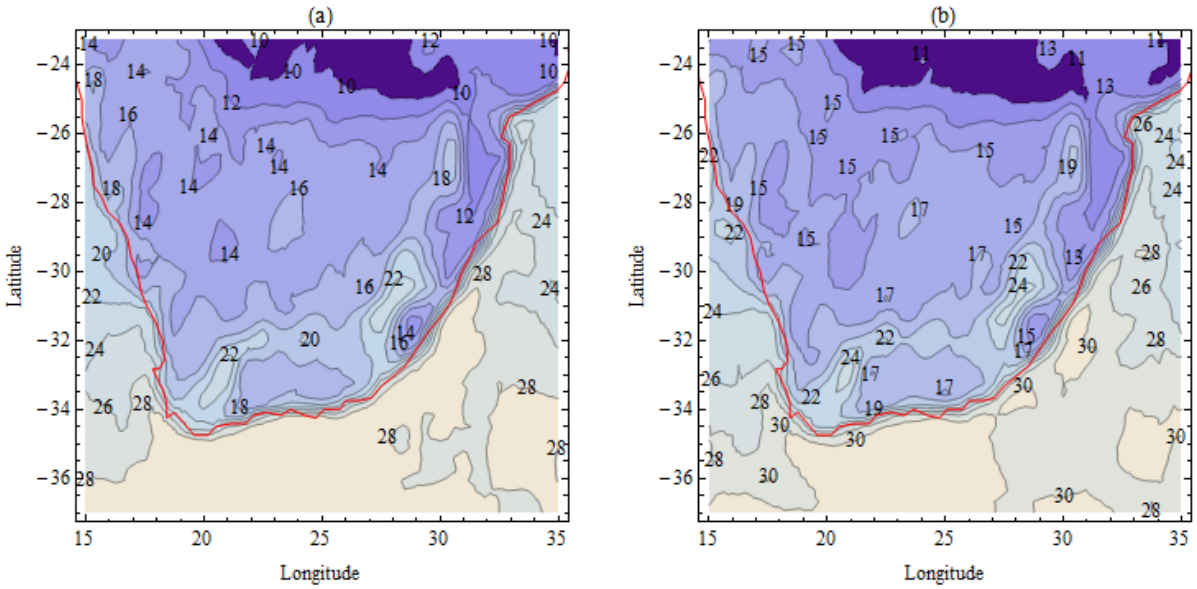

Figure 5. The 50-year wind U_{50} over South Africa, (a) from original time series of 1 hour resolution. (b) collected to 1 h resolution with full spectrum using the correction factor as in Figure 2a.

The inconsistency of the surface conditions between those described in the CSFR reanalysis and those corresponding to the measurements makes it a must to correct the modelled and measured winds to the same conditions. Since in reality, the roughness length over all measurement sites is close to 5 cm (Kruyer 2010), we only focus on calculations of the modelled extreme winds over the standard condition as explained in the introduction.

The atlases of $U_{50,st}$ were calculated and shown in Figure 6, where the four plots, a, b, c and d, represent the data and methods indicated in Table 1 as I, II, III and IV, respectively. The $U_{50,st}$ values are corrected to 1 hour using spectral correction.

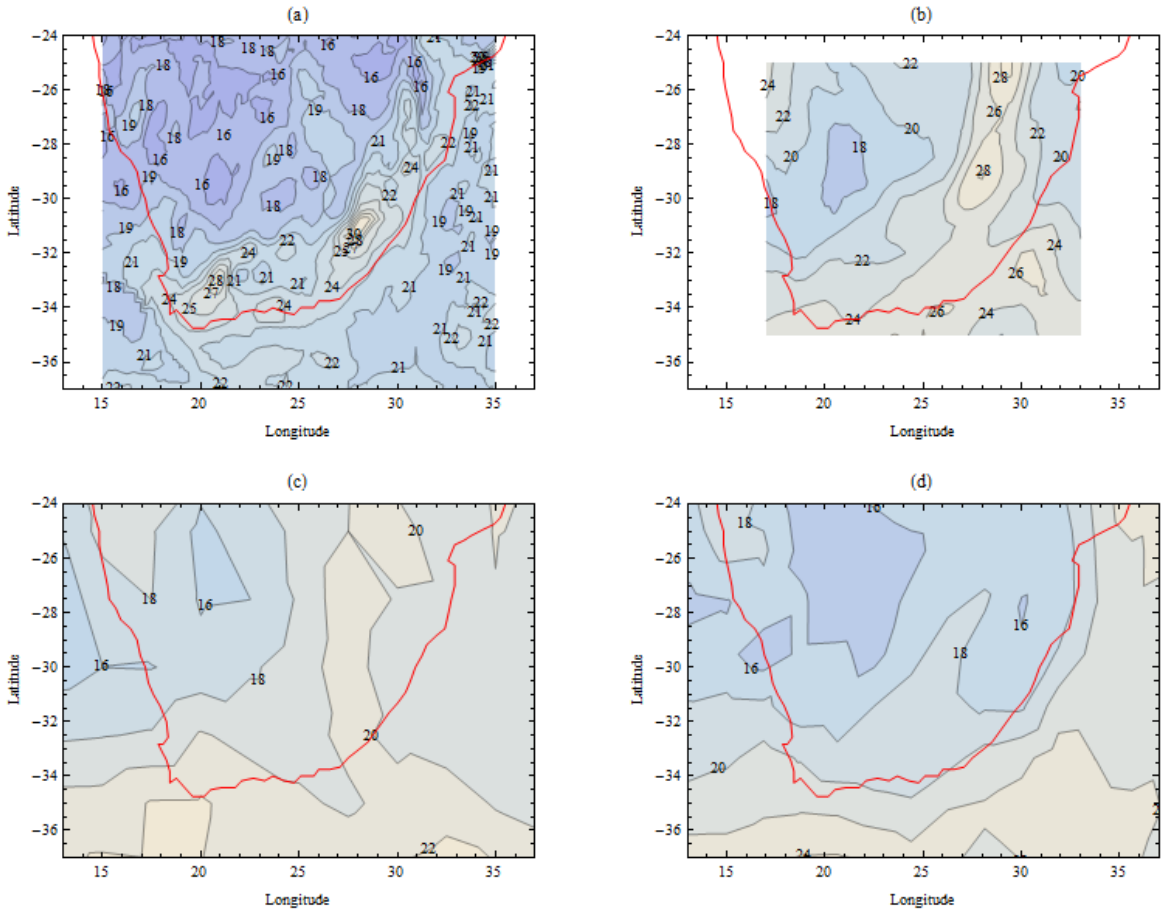

Figure 6. Atlases of $U_{50,st}$ of 1 h values corresponding to the combination of data and approach indicated in Table 1 as I, II, III and IV for a, b, c, and d, respectively.

The following observations can be made from Figure 6: (1) Different reanalysis with the same approach (b,c,d) suggest high extreme winds in the northern part between longitudes 27° and 30° in line with the high elevation to the right, with CFSR data showing the strongest (about 27 - 28 ms^{-1}) and NCEP-DOE data showing the weakest (about 20 ms^{-1}). The two reanalysis of coarser resolution, NCEP-DOE (d) and ERA-40 (c) are of comparable magnitude and they are systematically smaller than the results from CFSR data (b). It has not been explored if the differences in the magnitude of the maxima are related to the different spatial resolution of the different reanalysis data. (2) If the surface condition of Figure 6a is now more comparable to that in Figure 4a, the agreement is improved regarding the wind strength, although the maxima over the high elevation are only present in the CFSR data. This again could as well be due to too sparse measurements in these areas. (3) Both from the CFSR forecast data, but with completely different approaches, Figure 6a and b are consistent in several aspects, including the transition of generally weaker extreme winds from the west to the middle and to the east, as well as the wind strength. Figure 6a gives more spatial details. The strongest winds as suggested in Figure 6b and c around (-26°S, 29°E) are not present in Figure 6a. (4) Over simpler terrains (water and northwest part), the magnitude of the extreme winds in Figure 6a, 6c and 6d are rather similar.

6 Discussion, conclusions and future plan

We limited the extreme wind study to scales of 1 hour or greater. This, first of all, ruled out the complicated issues of multiple strong wind mechanisms (e.g. involvement of thunderstorms) which are rather common in some regions (Kruger 2010). Secondly, as Fig. 2b shows that on the scales of hours,

the dominant strong wind mechanisms are of rather large scales. This increases the credibility of using the coarse resolution modelled data.

The NCEP-DOE reanalysis and ERA-40 data, with the spectral correction, provide estimates of U_{50} with acceptable magnitude but miss details of the spatial distribution. The CFSR pressure data with Approach 1 (Figure 6b) has given extraordinary high values in the northeast part of the domain for which the cause is to be investigated. Seemingly, using the surface wind plus the generalization provides a more detailed spatial distribution of U_{50}, as expected from the measurements. Difficulties related to the generalization as stated in Larsén et al. (2012) remains in coastal areas, leading to large gradient of winds along the coastline, e.g. the Durban site on the east coast is an example: the values at 9 grid points around the site range from 19.1 to 28.5 m/s. This discontinuity of winds is considered as noise resulting from the uncertainty of the post-processing and it was smoothed out by averaging two layers[1] of grid points around each grid point on the coastline; the result is shown in Figure 6a.

For the CFSR data, extreme winds estimated with data from other two periods (1995 – 2010, 1998 – 2010) than those used for Figure 6a (1979 - 2010) were also examined. The two shorter time series gave similar results to each other, but, in addition to much higher fitting uncertainty due to small sample sizes, considerable differences between these two shorter period and Figure 6a are found over water. Without measurements over water, it is not possible at this stage to conclude which one is more reliable for offshore conditions.

For relatively complex terrains, the spatial wind variability of scales smaller than the reanalysis data resolution cannot be resolved. To address this issue, it is planned to run mesoscale model to capture the extreme wind episodes at much higher resolutions, such as a few kilometres. In addition, it is planned to improve the post-processing procedure for the generalization.

References

Badger J. et al. 2010: A universal mesoscale to microscale modelling interface tool, European Wind Energy Conference, Warsaw, Poland, 20 – 23 April.

Gumbel E.J. 1958. Statistics of Extremes. *Columbia University Press,* 51 pages.

Celliah M, Ebisuzaki W, Higgins W, Janowiak J, Mo KC, Ropelewski C, Wang J, Leetmaa A, Reynolds R, Jenne R,

Joseph D. The NCEP/NCAR 40-year reanalysis project. *Bulletin of the American Meteorological Society* 1996; **77**:437–471.

Kruger A.C., Goliger A., Retief J. and S. Sekele (2010), Strong wind climate zones in South Africa. Wind and Structure, Vol. 13, No 1.

Kruger A.C. (2010) *Wind climatology of South Africa relevant to the design of the built environment.* Unpublished PhD dissertation. Stellenbosch University.

Larsén X. G., & Mann, J. 2009. Extreme winds from the NCEP/NCAR reanalysis data. *Wind Energy* **12**, 556 – 573, Doi 10.1002/we.318.

Larsén X. G., Badger J., Hahmann A. N. & Mortensen N. G. 2012a. The selective dynamical downscaling method for extreme-wind atlases. *Wind Energy*, published online, Doi 10.1002/we.1544.

Larsén X. G., Ott S., Badger J., Hahmann A. N. & Mann J. 2012b. Recipes for correcting the impact of effective mesoscale resolution on the estimation of extreme winds. *J. Appl. Meteorol. Climat.*, 51: 521 – 533, Doi 10.1175/JAMC-D-11-090.1.

[1] "Averaging over two layers of grid points around each grid point on the coastline" means averaging points (I, J) where I = i – 2 to i + 2 and J = j – 2 to j + 2, given the coordinate of "the grid point on the coastline" is (i, j).

Larsén X. 2013: Extreme wind estimate for Hornsea wind farm. Wind Energy Report-I-0040. 30pp.

Saha et al. 2010a. The NCEP climate forecast system reanalysis. *American Meteorological Society.* DOI: 10.1175/2010BAMS3001.1.

Saha et al. 2010b. Supplement to The NCEP climate forecast system reanalysis. *American Meteorological Society*. DOI: 10.1175/2010BAMS3001.2.

Tennekes H. 1982. Similarity relations, scaling laws and spectral dynamics. In *Atmospheric turbulence and air pollution modelling*. Nieuwstadt FTM, van Dop H, (eds) D. Reidel publishing company: Dordrecht, 37 – 6.

Acknowledgement: This study is supported by the project "Wind Atlas for South Africa". The NCEP/NCAR reanalysis data are from www.cdc.noaa.gov. The ERA-40 data are obtained from http://www.ecmwf.int/. The CFSR data are from http://rda.ucar.edu/datasets/.